

Scale setting from a combination of lattice QCD formulations with Wilson and Wilson twisted mass valence quarks

Alejandro Saez-Gonzalvo,^{a,*} Alessandro Conigli,^{b,c} Gregorio Herdoiza^a and Carlos Pena^a

^a*Department of Theoretical Physics, Universidad Autónoma de Madrid, 28049 Madrid, Spain
and Instituto de Física Teórica UAM-CSIC, c/ Nicolás Cabrera 13-15 Universidad Autónoma de Madrid,
28049 Madrid, Spain*

^b*GSI Helmholtz Centre for Heavy Ion Research, Darmstadt, Germany*

^c*Helmholtz Institute Mainz, Johannes Gutenberg-Universität Mainz, 55099 Mainz, Germany*

*E-mail: alejandro.saezg@uam.es, aconigli@uni-mainz.de,
gregorio.herdoiza@uam.es, carlos.pena@uam.es*

We report about an update of a scale setting procedure employing a mixed action setup consisting of $N_f = 2 + 1$ flavors of $O(a)$ -improved Wilson sea quarks, based on CLS ensembles, and Wilson twisted mass valence quarks at maximal twist. We employ as external input isoQCD masses and decay constants of pions and kaons, and use the gradient flow scale t_0 as an intermediate scale. The analysis includes ensembles in the vicinity of the physical point and five values of the lattice spacing down to $a \approx 0.038$ fm. The determination of t_0 is carried out using three approaches: the unitary setup where Wilson quarks are used in the sea and valence sectors, the mixed action setup with Wilson twisted mass valence quarks, and by combining the data from the two previous cases. We observe that this combination leads to an improved control over the systematic uncertainties.

*The 41st International Symposium on Lattice Field Theory (LATTICE2024)
28 July - 3 August 2024
Liverpool, UK*

*Speaker

1. Introduction

The Standard Model of particle physics has been proven to describe a wide range of phenomena to a very high precision in modern day colliders. However, we know there must be some new physics at high energies. One way to search for new physics is by means of indirect searches, by reaching very high precision on both experimental and theoretical predictions, allowing to uncover small deviations between them. In this context, high precision theoretical calculations in the quark-flavor sector are of utmost importance, for which lattice field theory provides a first-principles method for calculating non-perturbative QCD contributions.

In this work we consider a lattice setup [1–5] aimed to address the leading systematic uncertainties affecting charm-quark observables. It is based on a mixed action regularization combining $N_f = 2 + 1$ Wilson quarks in the sea sector with $N_f = 2 + 1 + 1$ Wilson twisted mass in the valence sector which, when tuned to maximal twist, ensure $O(a)$ -improvement without the need of any improvement coefficient on physical observables, up to residual sea quark mass effects [2, 11, 12]. This key feature is of particular relevance when aiming at observables in the heavy quarks sector. In this work we present a study of the light – up, down, strange – quark sector, which is a necessary step of the analysis in the mixed action setup since a matching between the Wilson twisted mass (Wtm) valence and the sea of light quarks is needed. We set the scale of our lattice by use of the pion and kaon masses and decay constants as physical input, while using the gradient flow scale t_0 as intermediate scale.

2. Sea quark sector

Our sea quark sector consists in CLS gauge ensembles [9, 10] generated with $N_f = 2 + 1$ dynamical Wilson fermions, non-perturbatively $O(a)$ -improved. They employ open boundary conditions in time (OBC) for the gauge fields in order to avoid the problem of topology freezing as one approaches the continuum limit¹ [8].

These ensembles were generated following a chiral trajectory defined by

$$\text{Tr}(M_q^{\text{sea}}) = 2m_{ud}^{\text{sea}} + m_s^{\text{sea}} \approx \text{const}, \quad (1)$$

for the bare unsubtracted quark masses. We would like however this condition to hold for renormalized quark masses. For that purpose we define

$$\phi_4 = 8t_0 \left(m_K^2 + \frac{1}{2} m_\pi^2 \right), \quad (2)$$

with t_0 the gradient flow scale defined e.g. in [7], which we will employ as an intermediate scale in the scale setting analysis, and whose value at the physical point in physical units is the target of this work. This allows to rewrite Eq. (1) as (up to cutoff effects and higher order terms)

$$\phi_4^W \equiv \text{const}, \quad (3)$$

¹This is true except for two ensembles which are computed around the physical pion mass: E250 and D450, which employ periodic boundary conditions for the gauge fields.

where the superscript “W” refers to the value of the observable employing the Wilson fermionic fields of the sea sector. The value of the constant in Eq. (3) is given by the physical value of ϕ_4 .² In order to impose the condition on Eq. (3), it is necessary to perform small mass shifts in the observables of each ensemble under study. These shifts are achieved by using a low order Taylor expansion in the sea quark masses, according to the following expression

$$O(m_q'^{\text{sea}}) = O(m_q^{\text{sea}}) + \sum_q \delta m_q^{\text{sea}} \frac{dO}{dm_q^{\text{sea}}}, \quad (4)$$

where $\delta m_q^{\text{sea}} = m_q'^{\text{sea}} - m_q^{\text{sea}}$. In practice, we restrict the sum over the quark flavors \sum_q to $q = s$, as we found that doing so reduces the statistical uncertainty of the mass-shifted observables $O(m_q'^{\text{sea}})$. The value of δm_s^{sea} is chosen ensemble by ensemble such that condition Eq. (3) is satisfied.

The complete set of ensembles under study are presented in Table 1. In Fig. 1 we show the values of ϕ_4 for each ensemble under study before the mass-shifting procedure, in addition to the comparison between $\sqrt{8t_0}f_{\pi K}$ before and after mass-shifting.

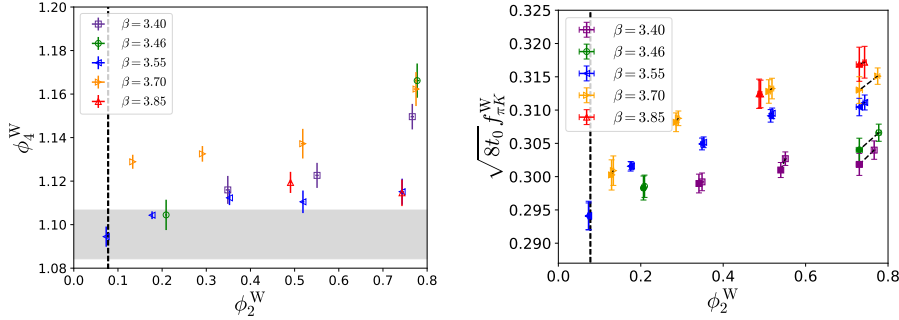


Figure 1: *Left:* Values of ϕ_4 in the sea sector for each ensemble, as a function of $\phi_2 = 8t_0m_\pi^2$ in the sea sector (“W”). We see the deviation from a constant value is at most $\sim 7\%$. The horizontal band represents the physical value ϕ_4^{ph} to which we wish to mass-shift the data, as determined from the final result of t_0^{ph} . *Right:* Comparison of $\sqrt{8t_0}f_{\pi K}$ before (empty symbols) and after (filled symbols) mass-shifting to impose $\phi_4 = \phi_4^{\text{ph}}$ in the sea sector as a function of ϕ_2 .

3. Valence quark sector

For the valence sector, we employ either the same regularization for the Dirac operator as in the sea quark sector, obtaining what we will refer to as a Wilson unitary setup; or a regularization based on Wilson twisted mass quarks [11, 12], obtaining the so-called mixed action regularization. The advantage of the latter is that when properly tuned at maximal twist, one obtains automatic $O(a)$ -improvement for any physical valence observable without the need of any improvement coefficient³

²Since in order to know the physical value of ϕ_4 we not only need m_π^{ph} , m_K^{ph} , but also t_0^{ph} , whose value is available only at the end of the scale setting analysis, we start with some initial guess for this quantity and iterate the analysis until convergence in t_0^{ph} is obtained. For the physical values of the pion and kaon masses we employ the reported values in [29].

³Up to residual $O(ag_0^4\text{Tr}(M_q^{\text{sea}}))$ cutoff effects coming from the sea. However, these are expected to have a negligible effect, given that the sea sector only involves light flavors.

β	a [fm]	id	m_π [MeV]	m_K [MeV]
3.40	0.086	H101	420	420
		H102	350	440
		H105	280	460
3.46	0.076	H400	420	420
		D450	222	480
3.55	0.064	N202	420	420
		N203	340	440
		N200	280	460
		D200	200	480
		E250	130	497
3.70	0.050	N300	420	420
		N302	340	440
		J303	260	470
		E300	176	496
3.85	0.038	J500	420	420
		J501	340	453

Table 1: $N_f = 2+1$ CLS ensembles [9, 10] used in the sea sector. These ensembles employ non-perturbatively $O(a)$ -improved Wilson fermions and open boundary conditions in the time direction for the gauge fields, except for E250 and D450, which use periodic boundary conditions.

[11, 12]. The explicit form of the Dirac operator employed in the valence Wtm regularization is

$$D_{\text{Wtm}} = D_{\text{W}} + \mathbf{m}^{\text{val}} + i\gamma_5 \boldsymbol{\mu}^{\text{val}}, \quad (5)$$

$$\mathbf{m}^{\text{val}} = \text{diag}(m_u, m_d, m_s, m_c)^{\text{val}}, \quad (6)$$

$$\boldsymbol{\mu}^{\text{val}} = \text{diag}(\mu_u, -\mu_d, -\mu_s, \mu_c)^{\text{val}}, \quad (7)$$

where D_{W} is the massless Wilson Dirac operator. In our setup, we will employ the same κ_q^{val} parameter for all quark flavors $q = u, d, s, c$, where κ_q is defined by

$$am_q = \frac{1}{2} \left(\frac{1}{\kappa_q} - \frac{1}{\kappa_{\text{cr}}} \right). \quad (8)$$

To achieve maximal twist, we impose a vanishing light (“12”) PCAC quark mass in the Wtm valence sector

$$am_{12}^{\text{Wtm}} \equiv 0, \quad (9)$$

which ensures (up to $O(a)$ cutoff effects) that maximal twist is also satisfied for any other quark flavor.

The use of a mixed action implies that unitarity is not satisfied even in the continuum limit unless the physical quark masses in the sea and valence sectors are tuned to be the same. This is imposed by means of a matching procedure.

4. Matching of the mixed action

In order to recover unitarity in the continuum limit in the context of a mixed action regularization, it is necessary to impose the condition that the physical quark masses in the valence sector are

equal to those in the sea sector. To this end, rather than examining renormalized quark masses, a similar condition is imposed on the pion and kaon pseudoscalar masses, or equivalently

$$\begin{aligned}\phi_2^W &\equiv \phi_2^{\text{Wtm}}, \\ \phi_4^W &\equiv \phi_4^{\text{Wtm}},\end{aligned}\tag{10}$$

where we defined

$$\phi_2 = 8t_0 m_\pi^2,\tag{11}$$

and where the superscript “W” refers to the value of the given observable in the Wilson unitary setup, which is the value for the corresponding observable in the sea sector; and “Wtm” refers to the value of the observable in the valence sector of the mixed action regularization.

In addition to Eq. (10), we need to impose Eq. (9) in order to ensure $\mathcal{O}(a)$ -improvement of valence observables. The way to impose these three conditions simultaneously is to employ a grid of values for the valence parameters of the Dirac operator, $(\kappa, a\mu_l, a\mu_s)^{\text{val}}$, along which we compute $(am_{12}^{\text{Wtm}}, \phi_2^{\text{Wtm}}, \phi_4^{\text{Wtm}})$, and which allows to interpolate to a point $(\kappa, a\mu_l, a\mu_s)^{\text{val},*}$ at which Eqs. (9)-(10) are satisfied. We illustrate such an interpolation in Fig. 2. Once this point in the parameter space is found, we compute the pion and kaon decay constants $f_{\pi,K}$ at such a point, which we will employ to set the scale.

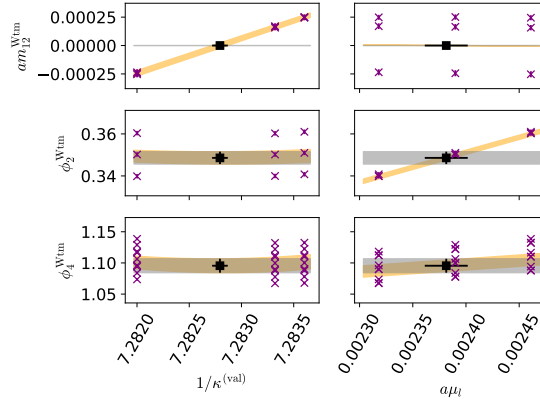


Figure 2: Matching of sea and valence sectors and tuning to maximal twist in the mixed action regularization. The colored crossed points represent the three relevant observables $am_{12}^{\text{Wtm}}, \phi_2^{\text{Wtm}}, \phi_4^{\text{Wtm}}$ along the grid of valence parameters $(\kappa, \mu_l, \mu_s)^{\text{val}}$. The orange band is the result of the fit along the grid, while the gray band is the value of the corresponding observables in the sea sector, as computed in the Wilson unitary setup. The black squared point marks the matching and maximal twist point.

5. Scale setting results

In order to define the physical point, we will use as physical external input the pion and kaon masses in the isoQCD limit as reported in [29], and the flavor average combination of pion and kaon decay constants

$$f_{\pi K} \equiv \frac{2}{3} \left(f_K + \frac{1}{2} f_\pi \right).\tag{12}$$

Their physical values in the isoQCD limit [29] will be employed to determine the gradient flow scale t_0 . To this end, the quantity $\sqrt{8t_0}f_{\pi K}$ was computed in both the Wilson unitary and mixed action setups. A chiral-continuum extrapolation was then performed to reach the continuum limit and the physical point $(\phi_2^{\text{ph}}, \phi_4^{\text{ph}})$.⁴ Universality arguments assert that both regularizations must share a common continuum limit. Consequently, in addition to conducting an independent analysis of the Wilson and mixed action regularizations, we also carry out a combined analysis by imposing a common continuum limit, while permitting distinct lattice artifacts for the two regularizations. This strategy improves the control of the continuum limit extrapolation, as the two regularizations approach the continuum limit from different directions (c.f. Fig. 3), while also increasing the statistical precision of the result.

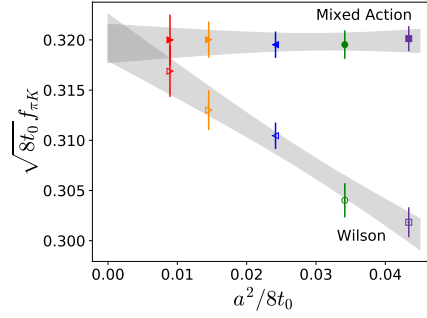


Figure 3: Continuum limit extrapolation of the symmetric point ensembles, which follow a line of constant physics defined by $\phi_4 = \phi_4^{\text{ph}}, \phi_2 = \frac{2}{3}\phi_4$. The lower, empty points come from the Wilson unitary setup, while the upper, filled points come from the mixed action setup. Each gray band is an independent fit to $O(a^2)$ cutoff effects, with no imposition to agree in the continuum limit.

To perform the chiral-continuum limit, we explore several possibilities. For the chiral extrapolation we consider SU(3) and SU(2) ChPT inspired ansätze, as well as Taylor expansions in ϕ_2 around the symmetric point defined by $\phi_2 = \frac{2}{3}\phi_4$. For the continuum limit, we consider $O(a^2), O(a^2\phi_2), O(a^2\alpha_s^{\Gamma_i}(1/a))$ cutoff effects⁵. Finally, in addition to different fit functions, we consider performing cuts in the data: removing the coarsest lattice spacing and thus keeping $\beta > 3.40$; removing the two coarsest and thus keeping $\beta > 3.46$; removing the heaviest pion, keeping $m_\pi < 420$ MeV; removing the two heaviest pions, keeping $m_\pi < 350$ MeV; removing both the coarsest lattice spacing and heaviest pion, keeping $\beta < 3.40, m_\pi < 420$ MeV; and removing the smallest volumes, keeping $m_\pi L > 4.1$. The impact of including these data subsets is explored by adding an extra term in the definition of the χ^2 function to be minimized by the fit. This ensures that when these data subsets are included, they receive an additional systematic uncertainty contribution in the χ^2 function so that they are not overweighted in the fit, with respect to the most chiral and continuum-like ensembles. By doing this, the model average gives a non-negligible weight to models that cut data, even if the greatest weights are still associated with no cuts.

⁴Note that thanks to the mass-shifting procedure, ϕ_4 was set equal to its physical value in a previous step of the analysis, and thus the chiral extrapolation is only performed in the ϕ_2 direction.

⁵For the $O(a^2\alpha_s^{\Gamma_i}(1/a))$ case, we test the different anomalous dimensions values Γ_i reported in [16], finding no real difference between choosing one or another for the final result, thus retaining only the smallest value $\Gamma_1 = -0.111$.

Subsequently, all these different models are averaged together using the Takeuchi's Information Criterion (TIC) [14]

$$\text{TIC} = \chi^2 - 2\chi_{\text{exp}}^2, \quad (13)$$

where χ_{exp}^2 is defined in [15], which allows to compute an averaged result for $\sqrt{t_0^{\text{ph}}}$ as

$$\left\langle \sqrt{t_0^{\text{ph}}} \right\rangle = \sqrt{t_{0,i}^{\text{ph}}} W_i, \quad (14)$$

$$W_i = A \exp\left(-\frac{1}{2}\text{TIC}_i\right), \quad (15)$$

where $\sqrt{t_{0,i}^{\text{ph}}}$ is the result for the scale coming from the i -th model, and A is a normalization constant such that $\sum_i W_i = 1$. Furthermore, the method assigns a systematic uncertainty to $\left\langle \sqrt{t_0^{\text{ph}}} \right\rangle$ given by

$$\sigma_{\text{syst}}^2 = \left\langle t_0^{\text{ph}} \right\rangle - \left\langle \sqrt{t_0^{\text{ph}}} \right\rangle^2. \quad (16)$$

In Fig. 4 we show the chiral-continuum extrapolation for the model including all data points, using SU(3) ChPT and $\mathcal{O}(a^2)$ cutoff effects, together with the model average for $\sqrt{t_0^{\text{ph}}}$, both for the combined analysis of the Wilson unitary and mixed action regularizations. We also show a comparison of our results with others in the literature. If instead of the reported values in [29] for the physical input of the pion and kaon masses and decay constants,

$$\begin{aligned} m_\pi &= 134.9768(5) \text{ MeV}, & m_K &= 497.611(13) \text{ MeV}, \\ f_\pi &= 130.56(2)_{\text{exp}}(13)_{\text{QED}}(2)_{|V_{ud}|} \text{ MeV}, & f_K &= 157.2(2)_{\text{exp}}(2)_{\text{QED}}(4)_{|V_{us}|} \text{ MeV}, \end{aligned} \quad (17)$$

we use those in [28],

$$\begin{aligned} m_\pi &= 134.8(3) \text{ MeV}, & m_K &= 494.2(3) \text{ MeV} \\ f_\pi &= 130.4(2) \text{ MeV}, & f_K &= 156.2(7) \text{ MeV}. \end{aligned} \quad (18)$$

to set the scale, we find an upwards shift in the central value of $\sqrt{t_0^{\text{ph}}}$ slightly below one sigma. Finally, if instead of the TIC we use other IC, as the one proposed in [13], for the combined analysis we find no significant impact in the final total error of $\sqrt{t_0^{\text{ph}}}$.

6. Conclusion

We have presented an update of the scale setting based on CLS ensembles, including physical point ensembles and lattice spacings all the way down to $a \approx 0.038$ fm. We have shown the effectiveness of combining the Wilson unitary and mixed action setups in order to enhance the statistical precision and improve the control of the continuum limit extrapolation, due to the fact that the considered regularizations approach the continuum with different lattice artifacts. Furthermore, we have explored the systematic effects associated to the chiral-continuum extrapolation and the inclusion of cuts in the data set. In the near future we plan to extend the scale setting analysis relying exclusively on physical external input of f_π . We refer to [6] for an application of the mixed action setup to the study of the charm quark mass.

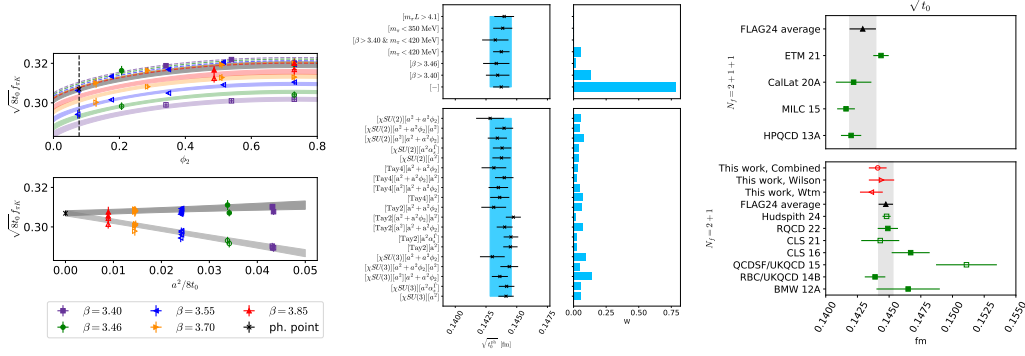


Figure 4: *Left:* Chiral-continuum extrapolation of $\sqrt{8}t_0 f_{\pi K}$ in the combined analysis of Wilson unitary and mixed action regularizations. A common mass-dependence in the continuum limit is imposed, while independent cutoff effects are allowed for the Wilson unitary (empty points) and mixed action (filled points) regularizations. The top panel shows the dependence on ϕ_2 , while the bottom one represents the continuum extrapolation, with all points projected to the physical pion mass. The vertical dashed line signals the value of ϕ_2^{ph} . *Middle:* Model variation and average for $\sqrt{t_0^{\text{ph}}}$. The blue vertical band represents the total averaged result, together with the systematic uncertainty as computed with Eq. (16). Weights are computed with Eq. (15). In the top panels, we show the model variation associated with the different cuts in data. To do so, we averaged together all models which employ the same number of data points but different fit functions. Tag “[−]” indicates no cut was performed. Conversely, in the bottom panels we averaged together all models which employ the same fit function, but different data cuts. All p-values are > 0.1 . The total systematic uncertainty amounts to $\sim 30\%$ of the total squared error. *Right:* Comparison of our determination of $\sqrt{t_0^{\text{ph}}}$ (red points) in the Wilson, mixed action, and combined analysis with other results in the literature [30]. We show our results for the Wilson, Wtm mixed action and combined analysis.

Acknowledgments

We are grateful to the Coordinated Lattice Simulations (CLS) initiative for the generation of the gauge field configuration ensembles employed in this study. We acknowledge PRACE for access to MareNostrum at Barcelona Supercomputing Center (BSC), Spain and to HAWK at GCS@HLRS, Germany. We thank CESGA for granting access to Finis Terrae II. We thank Emilio Ambite for technical support. This work is partially supported by grants PGC2018-094857-B-I00 and PID2021-127526NBI00, funded by MCIN/AEI/10.13039/501100011033 and by “ERDF A way of making Europe”, and by the Spanish Research Agency (Agencia Estatal de Investigación) through grants IFT Centro de Excelencia Severo Ochoa SEV-2016-0597 and No. CEX2020-001007-S, funded by MCIN/AEI/10.13039/501100011033. We also acknowledge support from the project H2020MSCAITN-2018-813942 (EuroPLEX), under grant agreement No. 813942, and the EU Horizon 2020 research and innovation programme, STRONG-2020 project, under grant agreement No. 824093.

References

- [1] G. Herdoíza, C. Pena, D. Preti, J. Á. Romero and J. Ugarrio, *A $tmQCD$ mixed-action approach to flavour physics*, *EPJ Web Conf.* **175** (2018), 13018, [1711.06017]

- [2] A. Bussone *et al.* [ALPHA], *Heavy-quark physics with a tmQCD valence action*, *PoS LATTICE2018* (2019), 270, [[1812.01474](#)].
- [3] J. Ugarrio *et al.* [Alpha], *First results for charm physics with a tmQCD valence action*, *PoS LATTICE2018* (2018), 271, [[1812.05458](#)].
- [4] A. Bussone *et al.* [ALPHA], *Matching of $N_f = 2 + 1$ CLS ensembles to a tmQCD valence sector*, *PoS LATTICE2018* (2019), 318, [[1903.00286](#)].
- [5] J. Frison, A. Bussone, G. Herdoíza, C. Pena, J. Á. Romero and J. Ugarrio, *Heavy semileptonic with a fully relativistic mixed action*, *PoS LATTICE2019* (2019), 234, [[1911.02412](#)].
- [6] A. Bussone *et al.* [Alpha], *Hadronic physics from a Wilson fermion mixed-action approach: charm quark mass and $D_{(s)}$ meson decay constants*, *Eur. Phys. J. C* **84** (2024), 506, [[2309.14154](#)].
- [7] M. Lüscher, *Properties and uses of the Wilson flow in lattice QCD*, *JHEP* **08** (2010), 071, erratum: *JHEP* **03** (2014), 092, [[1006.4518](#)].
- [8] M. Luscher and S. Schaefer, *Lattice QCD without topology barriers*, *JHEP* **07** (2011), 036, [[1105.4749](#)].
- [9] D. Mohler, S. Schaefer and J. Simeth, *CLS 2+1 flavor simulations at physical light- and strange-quark masses*, *EPJ Web Conf.* **175** (2018), 02010, [[1712.04884](#)].
- [10] M. Bruno, D. Djukanovic, G. P. Engel, A. Francis, G. Herdoiza, H. Horch, P. Korcyl, T. Korzec, M. Papinutto and S. Schaefer, *et al.* *Simulation of QCD with $N_f = 2 + 1$ flavors of non-perturbatively improved Wilson fermions*, *JHEP* **02** (2015), 043, [[1411.3982](#)].
- [11] R. Frezzotti and G. C. Rossi, *Chirally improving Wilson fermions. I. $O(a)$ improvement*, *JHEP* **08** (2004), 007, [[hep-lat/0306014](#)].
- [12] R. Frezzotti *et al.* [Alpha], *Lattice QCD with a chirally twisted mass term*, *JHEP* **08** (2001), 058, [[hep-lat/0101001](#)].
- [13] S. Borsanyi, Z. Fodor, J. N. Guenther, C. Hoelbling, S. D. Katz, L. Lellouch, T. Lippert, K. Miura, L. Parato and K. K. Szabo, *et al.* *Leading hadronic contribution to the muon magnetic moment from lattice QCD*, *Nature* **593** (2021), 51, [[2002.12347](#)].
- [14] J. Frison, *Towards fully bayesian analyses in Lattice QCD*, [2302.06550](#).
- [15] M. Bruno and R. Sommer, *On fits to correlated and auto-correlated data*, *Comput. Phys. Commun.* **285** (2023), 108643, [[2209.14188](#)].
- [16] N. Husung, *Logarithmic corrections to $O(a)$ and $O(a^2)$ effects in lattice QCD with Wilson or Ginsparg–Wilson quarks*, *Eur. Phys. J. C* **83** (2023), 142, erratum: *Eur. Phys. J. C* **83** (2023), 144 [[2206.03536](#)].

- [17] R. J. Hudspith, M. F. M. Lutz and D. Mohler, *Precise Omega baryons from lattice QCD*, [2404.02769](#).
- [18] G. S. Bali *et al.* [RQCD], *Scale setting and the light baryon spectrum in $N_f = 2 + 1$ QCD with Wilson fermions*, *JHEP* **05** (2023), 035, [[2211.03744](#)].
- [19] B. Strassberger, M. Cè, S. Collins, A. Gérardin, G. von Hippel, P. Korcyl, T. Korzec, D. Mohler, A. Risch and S. Schaefer, *et al.* *Scale setting for CLS 2+1 simulations*, *PoS LATTICE2021* (2022), 135, [[2112.06696](#)].
- [20] M. Bruno, T. Korzec and S. Schaefer, *Setting the scale for the CLS 2 + 1 flavor ensembles*, *Phys. Rev. D* **95** (2017), 074504, [[1608.08900](#)].
- [21] V. G. Bornyakov, R. Horsley, R. Hudspith, Y. Nakamura, H. Perlt, D. Pleiter, P. E. L. Rakow, G. Schierholz, A. Schiller and H. Stüben, *et al.* *Wilson flow and scale setting from lattice QCD*, [1508.05916](#).
- [22] T. Blum *et al.* [RBC and UKQCD], *Domain wall QCD with physical quark masses*, *Phys. Rev. D* **93** (2016), 074505, [[1411.7017](#)].
- [23] S. Borsányi *et al.* [BMW], *High-precision scale setting in lattice QCD*, *JHEP* **09** (2012), 010, [[1203.4469](#)].
- [24] C. Alexandrou *et al.* [Extended Twisted Mass], *Ratio of kaon and pion leptonic decay constants with $N_f=2+1+1$ Wilson-clover twisted-mass fermions*, *Phys. Rev. D* **104** (2021), 074520, [[2104.06747](#)].
- [25] N. Miller, L. Carpenter, E. Berkowitz, C. C. Chang, B. Hörz, D. Howarth, H. Monge-Camacho, E. Rinaldi, D. A. Brantley and C. Körber, *et al.* *Scale setting the Möbius domain wall fermion on gradient-flowed HISQ action using the omega baryon mass and the gradient-flow scales t_0 and w_0* , *Phys. Rev. D* **103** (2021), 054511, [[2011.12166](#)].
- [26] A. Bazavov *et al.* [MILC], *Gradient flow and scale setting on MILC HISQ ensembles*, *Phys. Rev. D* **93** (2016), 094510, [[1503.02769](#)].
- [27] R. J. Dowdall, C. T. H. Davies, G. P. Lepage and C. McNeile, *Vus from pi and K decay constants in full lattice QCD with physical u, d, s and c quarks*, *Phys. Rev. D* **88** (2013), 074504, [[1303.1670](#)].
- [28] S. Aoki, Y. Aoki, D. Becirevic, C. Bernard, T. Blum, G. Colangelo, M. Della Morte, P. Dimopoulos, S. Dürr and H. Fukaya, *et al.* *Review of lattice results concerning low-energy particle physics*, *Eur. Phys. J. C* **77** (2017), 112, [[1607.00299](#)].
- [29] Y. Aoki *et al.* [Flavour Lattice Averaging Group (FLAG)], *FLAG Review 2021*, *Eur. Phys. J. C* **82** (2022), 869, [[2111.09849](#)].
- [30] Y. Aoki *et al.* [Flavour Lattice Averaging Group (FLAG)], *FLAG Review 2024*, [2411.04268](#).